RSC Advances

Cite this: *RSC Advances*, 2012, **2**, 9952–9957

www.rsc.org/advances

PAPER

New self-assembled supramolecular polymers formed by self-complementary sextuple hydrogen bond motifs†

Chih-Chia Cheng,[a] I-Hong Lin,[a] Ying-Chieh Yen,[a] Chih-Wei Chu,[bc] Fu-Hsiang Ko,[d] Xinling Wang[e] and Feng-Chih Chang*[af]

Received 25th May 2012, Accepted 19th August 2012
DOI: 10.1039/c2ra21039h

A new supramolecular material, *N*-(6-(3-(2,4-dioxo-3,4-dihydropyrimidin-1(2*H*)-yl)propanamido)pyridin-2-yl)undec-10-enamide (U-DPy) possesses an extremely high association constant (K_a >10^7 M^{-1}), which is able to dimerize through a self-complementary sextuple hydrogen-bonding array. As the end groups of an oligomer, U-DPy forms a self-assembling polymer system. These new mono- and difunctional telechelic supramolecular polymers have highly prominent properties, leading to a substantial increase in viscosity, thermal stability and unique morphology changes in the solid state. More surprisingly, they can self-organize into lamellar crystallization and a spherical structure. In addition, upon increasing the concentration in the solution state, the size of the resulting spherical structure is gradually increased. These spherical structures are constructed from supramolecular polymers with a high degree of polymerization.

Introduction

Supramolecular materials permit a rapid response to a change in environment, resulting in easily controllable strength and selectivity of noncovalent interactions. A typical example is the assembling and disassembling[1] of structural motifs such as DNA—fundamental for translation and transcription in biology. Formation of polymers or polymer networks *via* noncovalent interactions is therefore an attractive approach to constructing stimuli-responsive soft materials.[2,3] Recently, supramolecular chemistry has evolved to a stage where the paradigm can be explored, with building blocks now widely available that (a) are easy to make in multi-gram quantities and (b) interact in a defined manner with sufficient strength.

Since Carothers *et al.* established his influential theory on polymerization 81 years ago,[4] there have been numerous synthetic approaches to obtain high-molecular-weight polymers through condensation polymerization.[5] Condensation polymers all have two properties in common—staticity and nonreversibility, either in the polymerization process or in the cross-linking process. Indeed, sequentially reversible polymers are difficult to synthesize through covalent bonds, but similar architectures can be achieved through strong noncovalent interactions, utilizing highly complementary noncovalent bonds.[6] To these polymers, the simplest structure is derived from hydrogen-bonded polymers in which the proton donor and acceptor groups are located in separate oligomer main chains or chain ends, allowing the new supramolecular polymer to be produced without covalent polymerization.[7] Recently, several supramolecular structures have been incorporated into polymers to form materials with the features of conventional polymers and reversibility in the bonding between monomer units.[8] By choosing the appropriate hydrogen bonding motif, strength of bonding with a binding constant larger than 10^6 M^{-1} can be obtained, which is close to the strength of conventional covalent linkages.[1,7] Meijer and co-workers[9,10] established a series of supramolecular polymers exhibiting mechanical properties that were thought to be reachable only by covalently linked monomers in macromolecules. In addition, Lehn[11] and Binder[12] used the hydrogen bonding motif for preparing chain-extended supramolecular polymers and block copolymers, which can assemble *via* a strong six-point hydrogen bond association. Nevertheless, it is still a challenge to control the non-covalent polymers with secondary (and higher) bonding from different hydrogen-bonding motifs.[13,14]

Our recent findings[15] indicate that a new derivative of *N*-(6-(3-(2,4-dioxo-3,4-dihydropyrimidin-1(2*H*)-yl)propanamido)pyridin-2-yl)undec-10-enamide (U-DPy) can dimerize easily and strongly by means of a self-complementary DADADA (donor–acceptor–donor–acceptor–donor–acceptor) array of sextuple hydrogen

[a]*Institute of Applied Chemistry, National Chiao-Tung University, Hsinchu 30050, Taiwan. E-mail: changfc@mail.nctu.edu.tw; Fax: +886-3-5131512*
[b]*Research Center for Applied Sciences, Academia Sinica, Taipei 11529, Taiwan*
[c]*Department of Photonics, National Chiao-Tung University, Hsinchu 30050, Taiwan*
[d]*Department of Materials Science and Engineering, National Chiao-Tung University, Hsinchu 30050, Taiwan*
[e]*School of Chemistry & Chemical Technology, Shanghai Jiao Tong University, Shanghai 200240, P. R. China*
[f]*Department of Materials and Optoelectronic Science, National Sun Yat-Sen University, Kaohsiung 80424, Taiwan*
† Electronic Supplementary Information (ESI) available. See DOI: 10.1039/c2ra21039h

bonding interactions. ^{1}H NMR titration studies in $CDCl_3$ showed that the self-complementary complexes formed rapidly on the NMR time scale with extremely high association constants ($K_{dimer} > 10^7$ M^{-1}). More surprisingly, the strength of hydrogen bonding formed through dimerization was over the fluorescence time scale, prompting us to this functionality as an end group in reversible self-assembling polymer systems. To the best of our knowledge, this is the first example of the formation of a U-DPy-based supramolecular polymer in which the new polymer possesses polymeric properties in the solution as well as in the bulk state.

Results and discussion

Synthesis and viscosity behavior of the U-DPy telechelic supramolecular polymer

We present here a general route for preparing well-defined, end-functional U-DPy polymers of controlled molecular architectures, attainable through supramolecular polymerization from strongly associating U-DPy functional groups. Polyethylene glycol (PEG) was chosen as the polymer backbone due to its wide application areas in the chemical, biomedical, and industrial fields. Two low molecular weight oligomers, mono- and dipropargyl terminated PEG 1000, were functionalized by the click reaction with azide-labeled U-DPy (N3-U-DPy) in high yields (>90%). The products are U-DPy-PEG1T and BU-DPy-PEG1T, whose structures are shown in Fig. 1a (detailed synthetic strategy is described in the ESI†). Most importantly, the variable-temperature NMR (VT-NMR) experiments of MU-DPy-PEG1T and BU-DPy-PEG1T in tetrachloroethane-d_2 (shown in Fig. S5a and S5b, ESI†) obtained at 30 °C show a clear downfield peak (12.61 ppm) for the N–H proton (of the uracil units), which corresponds to the formation of the selective hydrogen bonded complex between uracil and diamidopyridine (DAP).[15] When these samples were heated from 30 to 120 °C, the peak of the amide proton was shifted slightly upfield from 12.61 to 11.91 ppm. This indicates that the hydrogen bonding interaction is not appreciably destroyed during heating, which was rarely observed. In these previous studies, the multiple hydrogen bonding systems were significantly influenced by an increase in temperature, showing an obvious shift of amide proton signals.[16,17] In addition, we also performed VT-NMR on azide-labeled U-DPy (a precursor for the synthesis of U-DPy-modified polymers) and a similar trend was seen for MU-DPy-PEG1T and BU-DPy-PEG1T (Fig. S6†). This observation further indicates that the U-DPy PEG system forms highly stable hydrogen-bonded complexes in tetrachloroethane. To further evaluate the effect of hydrogen-bonding associations on solution viscosity, the viscosities of MU-DPy-PEG1T and BU-DPy-PEG1T in chloroform at ambient temperature were measured using an Ubbelohde viscometer (Fig. 1b). The viscosity of the BU-DPy-PEG1T increased nonlinearly with concentration. When the concentration is below 66 mg dL^{-1}, the slope of the line is calculated as 0.0917, while above the critical concentration the slope becomes 0.46. This result indicates that the concentration dependent association between the individual monomer units is significantly greater than both PEG 20 000 and MU-DPy-PEG1T, even though the PEG 20 000 has a higher molecular weight with more entanglements. These results from BU-DPy-PEG1T may come from the equilibrium between the linear polymeric and oligomeric cyclic structures (Scheme 1). In other words, raising the BU-DPy-PEG1T concentration induces the transition from the kinetically favorable *intra-molecular* interaction (at low concentration) to the dynamically favorable *intermolecular* hydrogen bonding interaction (at high concentration) and results in an increase in the degree of polymerization.[10]

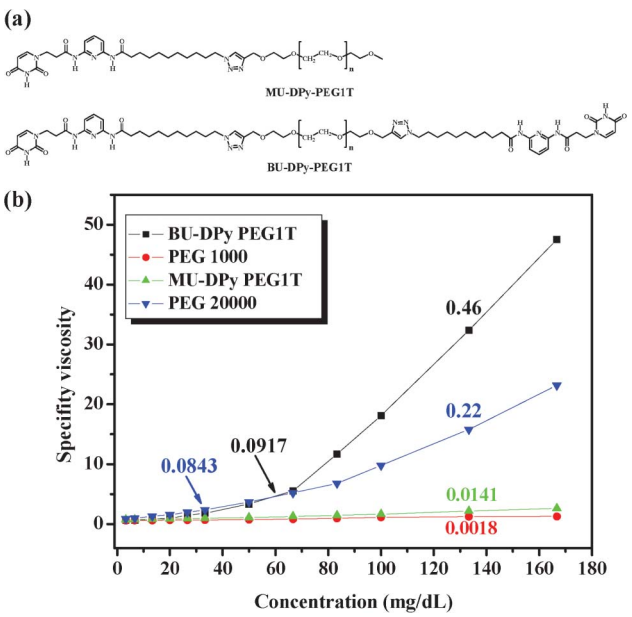

Fig. 1 (a) Chemical structures of the U-DPy telechelic supramolecular polymer. (b) Specific viscosity of MU-DPy-PEG1T, BU-DPy-PEG1T and the control PEG *versus* concentration in $CHCl_3$ at 25 °C.

Polymer-like behavior

Phase behaviors of MU-DPy-PEG1T and BU-DPy-PEG1T were investigated by wide angle X-ray scattering (WAXS) and differential scanning calorimetry (DSC). Fig. 2a presents the WAXS data of MU-DPy-PEG1T and BU-DPy-PEG1T. MU-DPy-PEG1T exhibits several sharp peaks because of its crystalline structure. The attachment of the difunctional U-DPy to the PEG chain ends led to the disappearance of these sharp peaks, and replacement by a broad amorphous halo centered at q = 14.4 (d = 0.44 nm), indicating that the U-DPy groups on the chain ends possess a steric effect, to hinder the formation of crystalline PEG. Moreover, the WAXS pattern displays a reflection peak at

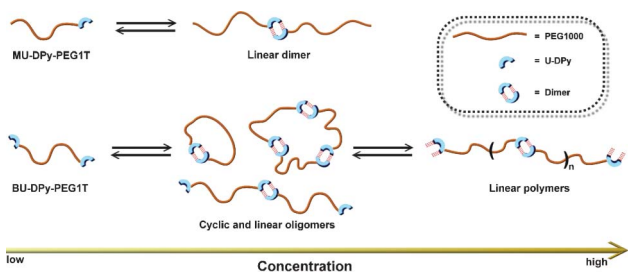

Scheme 1 Schematic representation of the supramolecular polymerization obtained from mono- and difunctional U-DPy derivatives, respectively, as a function of concentration.

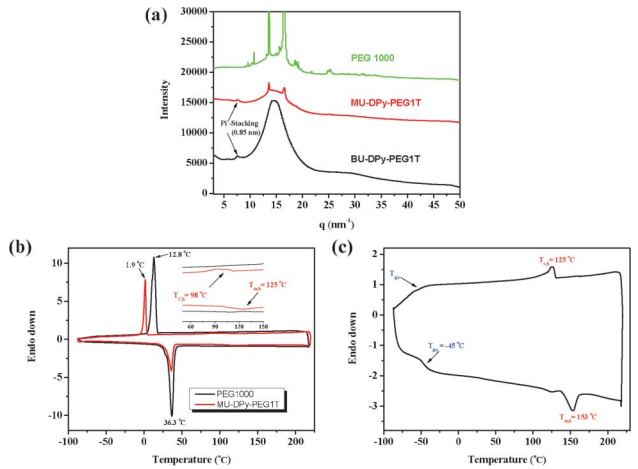

Fig. 2 (a) WAXS data for annealing MU-DPy-PEG1T, BU-DPy-PEG1T and the control PEG 1000. DSC curves of (b) MU-DPy-PEG1T and (c) BU-DPy-PEG1T.

q = 7.35 (d = 0.85 nm), suggesting that there are stacks of the dimer that are held together through π–π interactions within the domain formed by U-DPy, as shown in Fig. 2a.[15] In the DSC curves shown in Fig. 2b and 2c, MU-DPy-PEG1T exhibits a sharp melting point (T_m) at 36.3 °C, whereas BU-DPy-PEG1T displays a clear glassy transition (T_g = −45 °C) and a melting point ($T_{m,h}$ = 125 °C), which can be attributed to the supramolecular binding motif in the bulk playing a critical role in affecting the phase segregation between the U-DPy and PEG chains.[17,18]

Interestingly, the MU-DPy-PEG1T shows a lower crystallization peak (T_c = 1.9 °C) than the control PEG 1000 (T_c = 12.8 °C), probably due to the association of certain units affecting the crystallization behavior.[19] This intriguing behavior leads us to investigate microstructures of this phenomenon in more detail through isothermal crystallization kinetics and atomic force microscopy (AFM) measurements. The typical

(a)

Samples	Temperature (K)	n	K	$t_{1/2}$ (min)
PEG1000	283	1.9019	0.51662	1.13
	286	1.94145	0.49386	1.25
	289	1.81071	0.49282	1.31
	292	1.76873	0.30692	1.64
MU-DPy-PEG1T	283	2.20266	0.23205	0.87
	286	2.31886	0.01238	4.61
	289	2.53584	0.00029	20.52
	292	2.11625	0.00004	112.88

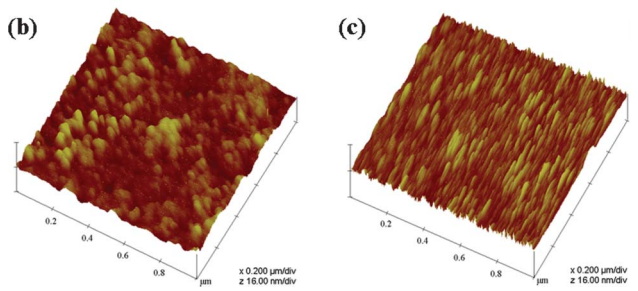

Fig. 3 (a) The table presents the kinetic data and (b, c) AFM images showing the spherical and lamellar crystal morphology of annealed (b) PEG 1000 and (c) MU-DPy-PEG1T, respectively.

isotherm data (Fig. 3a) of MU-DPy-PEG1T and control PEG 1000 indicate that introducing a U-DPy end group results in a significant reduction of the overall kinetic rate constant (K), and the crystallization rate is progressively decreased. In addition, the Avrami exponents (n) of MU-DPy-PEG1T are around 2.1–2.5, which is higher than PEG 1000. This result reveals the presence of two-dimensional crystallization[20] and stacks of dimerized U-DPy moieties affecting the crystallization morphology. To further confirm the isotherm results, we performed an AFM experiment to visually observe the crystal structure of MU-DPy-PEG1T. As shown in Fig. 3b, the PEG 1000 exhibits a typical spherulite morphology. In contrast, MU-DPy-PEG1T forms lamellar objects instead of spherical objects (Fig. 3c), suggesting that the PEG crystals grow preferentially in some directions due to the presence of the U-DPy end group. As well as the isotherm data, the AFM images also revealed that this MU-DPy-PEG1T system exhibits the strongest segregation strength and results in a stable and confined crystallization in the lamellar arrangement.

Self-assembly of BU-DPy-PEG1T in the bulk state

Supramolecular self-assembly can be used as a bottom-up approach for the development of advanced structures.[21] If these hydrogen bonds are strong enough, supramolecular polymerization can refer to the objects directly.[22] We performed variable-temperature small-angle X-ray scattering (SAXS) and atomic force microscopy (AFM) to understand the self-assembly behavior of BU-DPy-PEG1T. Fig. 4a displays the SAXS profiles of BU-DPy-PEG1T at 25 °C. Surprisingly, annealing BU-DPy-PEG1T resulted in the appearance of an ordered regularization. Highly ordered lamellar microstructures are observed (n = 1–3) with the first intense reflection at q = 1.10 nm^{-1} corresponding to a spacing of d = 5.71 nm. Upon heating from 25 to 150 °C, the SAXS profile remains nearly unchanged, as shown in Fig. 4a, implying that BU-DPy-PEG1T forms highly stable lamellar structures in the bulk state.[23,24] In addition, the one-dimensional correlation function is employed to analyze the detailed structural information (Fig. 4b) and determine the most probable average length period (L), the average crystalline lamellar thickness (L_1) and the average interlamellar amorphous layer thickness (L_2). Based on the self-correlation triangle method, the mean thickness of L_1 is 1.51 nm and the mean thickness of L_2 from $L_2 = L - L_1$ (5.71 − 1.51 = 4.20 nm) is 4.20 nm, which is constructed on lamellae microstructures as depicted in Scheme 2. Accordingly, the lamellar structures are formed by the PEG region of 4.2 nm in length, connected side by

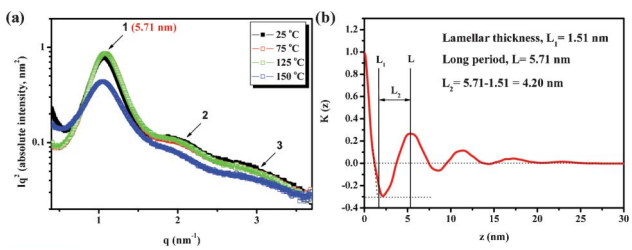

Fig. 4 (a) One-dimensional SAXS data and (b) one-dimensional correlation function calculated from the SAXS data for BU-DPy-PEG1T recorded at room temperature.

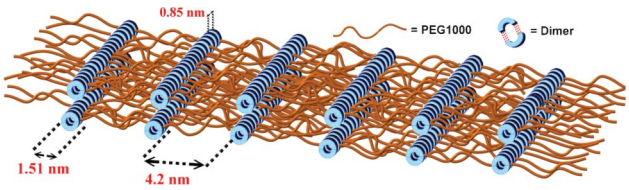

Scheme 2 Graphical representations of the lamellar structures of the BU-DPy-PEG1T self-complexes in the bulk state.

side with the dimerized U-DPy moieties (1.51 nm). In addition, the close π-packing of these lamellae with a *d* spacing of 0.85 nm (Fig. 2a) also facilitates the system to form stable structures. On other hand, spherical particles were observed from AFM with samples prepared by dropping chloroform solutions of BU-DPy-PEG1T in different concentrations onto wafer surfaces, followed by drying and annealing (Fig. 5a–d). More surprisingly, the gradual increase in particle size with increasing concentration can be stabilized to maintain spherical structures throughout its growth (Fig. 5e). Remarkably, it can exist as a stable 'zero-dimensional' nanostructure based on these observations, rather like the previous reports found in fibrous or higher structures.[18,25,26] These results also confirmed that BU-DPy-PEG1T was indeed present in unimolecular micelles. In addition, we found that sextuple hydrogen bonding alone is enough to permit assembly of the chain into a well-defined particle.

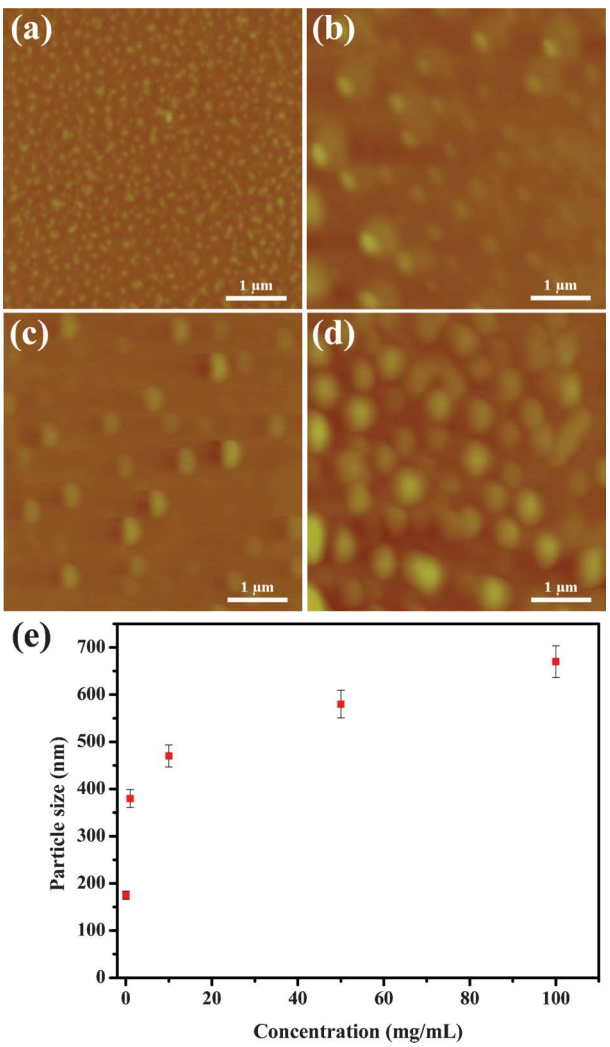

Fig. 5 AFM images of annealed BU-DPy-PEG1T on the wafer surface with different concentrations: (a) 0.0067, (b) 1, (c) 10 and (d) 100 mg mL^{-1}. (e) Particle size of annealed BU-DPy-PEG1T *versus* concentration as measured by AFM.

To further evaluate the propensity of the new module for spherical growth, diffusion coefficient (*D*) measurements in 16.7 and 167 mg dL^{-1} solutions of BU-DPy-PEG1T in $CDCl_3$ were undertaken in order to analyze the degree of self-association in different concentrations. For the solution with a concentration of 16.7 mg dL^{-1}, the diffusion coefficient is calculated to be 2.35×10^{-10} m^2 s^{-1}, indicating the presence of cyclic oligomers in dilute chloroform solutions.[10] Further polymerization occurs upon increasing the concentration, as confirmed by an extremely slow diffusion, with a *D* value of 9.81×10^{-12} m^2 s^{-1} for 167 mg dL^{-1}, implying a high degree of polymerization for BU-DPy-PEG1T. In addition, the DP of the supramolecular polymer was calculated to be approximately 146 at a concentration of 167 mg dL^{-1}.[27] Diffusion coefficient measurements also agree well with the viscosity results (Fig. 1b).

With these data in hand, the growth mechanism of the spherical structure can be easily explained *via* the Flory–Huggins theory.[28] This theory predicts the transition of cylindrical aggregation to micellar aggregation with an increase in the volume fraction of spherical aggregation.[29] In other words, the morphology from zero-dimensional growth at very dilute concentrations can be attributed to the clustering of cyclic oligomers[30] and the formation of small particles (Fig. 5a and Scheme 3). In contrast, large particles formed at high concentration—presumably by clustering of linear polymers[31] (Fig. 5d and Scheme 3), which constructed supramolecular polymers with a high degree of polymerization. These results also demonstrate the morphological nature of the collapsed particle state. As observed by Brus and coworkers, the self-assembled morphologies can be modeled with increasing domain size on the surface, and are in good agreement with our results.[32] Ultimately, this work presents a new phenomenon to an elusive target: incorporation of D-UPy units into polymers can be turned into a high-performance supramolecular material.

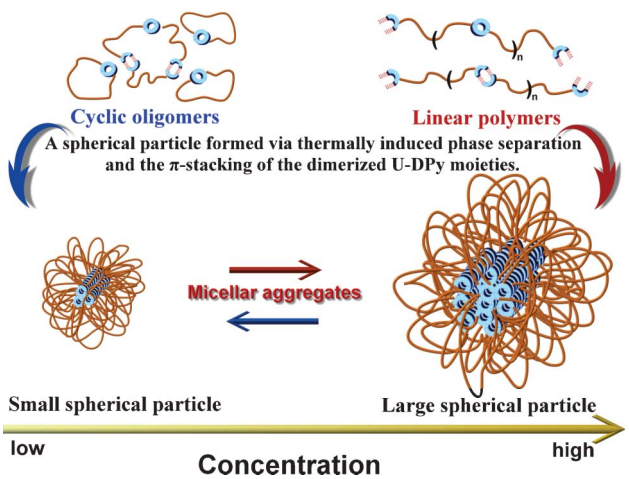

Scheme 3 Suggested processes of the formation of the micellar aggregations in the bulk state.

Conclusions

In summary, we have demonstrated that the recognition units possessing extremely high K_a lead to new supramolecular polymers in the bulk as well as in solution. Incorporation of U-DPy units into PEG chain ends results in phase separation, dramatically changed morphology and formation of a supramolecular complex chain with an extremely high degree of polymerization. In addition, the U-DPy telechelic derivative possesses polymer-like properties as a result of self-complementary interactions, providing a potential route toward the design and fabrication of polymer-like supramolecular materials.

Experimental section

Materials

All other chemicals were purchased from Aldrich (USA) or Acros Organics (Germany) and were used as received. All solvents were purchased from TEDIA (USA) and distilled over CaH_2 prior to use.

Syntheses of supramolecular polymers

MU-DPy-PEG1T and BU-DPy-PEG1T were prepared by "click chemistry" of U-DPy azide in the presence of propargyl PEG 1000 using CuBr/PMDETA as the catalyst system. The general materials in this work are described in more detail in the ESI.†

Characterizations

Viscosity experiment. The effects of hydrogen-bonding associations on solution viscosities of MU-DPy-PEG1T and BU-DPy-PEG1T in $CHCl_3$ solution at ambient temperature were measured using an Ubbelohde viscometer.

Nuclear magnetic resonance (NMR) measurement. ^{1}H-NMR spectra were recorded using a Varian Inova-500 MHz spectrometer equipped with a 9.395 T Bruker magnet. Samples of *ca.* 5 mg were analyzed at 25 °C in deuterated solvent. ^{13}C-NMR spectra were obtained on a Varian Inova- 500 MHz spectrometer operated at 125 MHz. All samples of *ca.* 20 mg were dissolved in deuterated solvent and analyzed at 25 °C.

Elemental analysis (EA). The carbon, hydrogen, and nitrogen contents of the samples were obtained using a CHN-*O*-Rapid elemental analyzer (Foss. Heraeus, Germany).

Dynamic light scattering (DLS). DLS measurements were conducted using a 90Plus laser particle size analyzer (Brookhaven Instruments Corp., USA), which was calibrated using a 60 nm latex standard. The scattering from a small amount of the sample dissolved in chloroform was measured at 90°. The hydrodynamic radius (r) of the aggregates was calculated using the Stokes–Einstein equation: $r = k_BT/6\pi\eta D$, where k_B is the Boltzmann constant, T is the absolute temperature, η is the solvent viscosity, and D is the diffusion constant.

FT-IR spectroscopy. Recorded using a Nicolet Avatar 320 FT-IR spectrometer; 32 scans were collected at a spectral resolution of 1 cm^{-1}. The conventional KBr disk method was employed: the sample was dissolved in chloroform and then cast onto a KBr disk and dried under vacuum at 70 °C.

Polarized optical microscopy. The cover glass containing the sample film was placed under a polarized optical microscope (Olympus BX51) equipped with a camera system.

Differential scanning calorimetry (DSC). DSC was performed using a TA DSC-Q20 controller operated under a dry nitrogen atmosphere. The samples were weighed (*ca.* 5–10 mg), sealed in an aluminum pan, and then heated and cooled from −90 to +240 °C at a rate of 10 °C min^{-1}.

Wide angle X-ray scattering (WAXS). WAXS was collected by the 01C2 SWLS beamline of the National Synchrotron Radiation Research Center (NSRRC), Taiwan. For the experiment, radiation with a wavelength of 0.103316 nm was used. The beam possessed a diameter of 100 mm at the sample position, which was defined by a pinhole collimator. All tests were performed at ambient conditions (23 °C, 65% relative humidity).

Small-angle X-ray scattering (SAXS). SAXS data were collected using the BL17A1 wiggler beamline of the National Synchrotron Radiation Research Center (NSRRC), Taiwan. The samples were sealed between two Kapton windows (thickness: 12 μm) and measured at room temperature. An X-ray beam with a diameter of 0.5 mm and a wavelength (λ) of 1.1273 Å was used for the SAXS measurement (Q range: 0.015–0.3 Å^{-1}). The Q values of the SAXS profiles were calibrated using a polyethylene standard, Ag behenate, and tripalmitat.

Atomic force microscopy (AFM). Height measurements of the microcapsules were determined using tapping-mode AFM (Digital Instrument NS4/D3100CL/Multi- Mode AFM; Veeco-Digital Instruments, Santa Barbara, CA) with silicon cantilevers (Pointprobe Silicon AFM Probe) at 25 °C in air. The samples for AFM investigation were prepared by placing a drop of the sample solution onto a wafer substrate and then evaporating the solvent (chloroform).

Diffusion NMR experiments. Diffusion coefficients were recorded on a Bruker NMR spectrometer, AMX400. Full details of diffusion NMR experiments (all at 298 K) were performed as in the procedures described previously.[33] A convection compensated pulse sequence was used in this work.[34]

Acknowledgements

We thank National Synchrotron Radiation Research Center (NSRRC, Taiwan) for the support in the SAXS measurement. This study was supported financially by the National Science Council, Taiwan (contract no. NSC 99-2120-M-009-008).

References

1 D. Philp and J. F. Stoddart, *Angew. Chem., Int. Ed. Engl.*, 1996, **35**, 1155.
2 A. Ciferri, *Supramolecular Polymers*, 2nd edn, Taylor and Francis, Boca Raton, Florida, 2005.
3 L. Brunsveld, B. J. B. Folmer, E. W. Meijer and R. P. Sijbesma, *Chem. Rev.*, 2001, **101**, 4071.

4 W. H. Carothers, *Chem. Rev.*, 1931, **8**, 353.
5 G. Odian, *Principles of Polymerization*, Wiley, New York, 1991.
6 J.-M. Lehn, *Aust. J. Chem.*, 2010, **63**, 611.
7 S. Sivakova and J. Rowan, *Chem. Soc. Rev.*, 2005, **34**, 9.
8 J. D. Fox and S. J. Rowan, *Macromolecules*, 2009, **42**, 6823.
9 O. A. Scherman, G. B. W. L. Ligthart, H. Ohkawa, R. P. Sijbesma and E. W. Meijer, *Proc. Natl. Acad. Sci. U. S. A.*, 2006, **103**, 11850.
10 O. A. Scherman, G. B. W. L. Ligthart, R. P. Sijbesma and E. W. Meijer, *Angew. Chem., Int. Ed.*, 2006, **45**, 2072.
11 E. Kolomiets and J.-M. Lehn, *Chem. Commun.*, 2005, 1519.
12 W. H. Binder, S. Bernstorff, C. Kluger, L. Petraru and M. J. Kunz, *Adv. Mater.*, 2005, **17**, 2824.
13 M. Muthukumar, C. K. Ober and E. L. Thomas, *Science*, 1997, **277**, 1225.
14 B. Gole, S. Shanmugaraju, A. K. Bar and P. S. Mukherjee, *Chem. Commun.*, 2011, 10046.
15 C. C. Cheng, Y. C. Yen and F. C. Chang, *RSC Adv.*, 2011, **1**, 1190.
16 E. Kolomiets, E. Buhler, S. J. Candau and J.-M. Lehn, *Macromolecules*, 2006, **39**, 1173.
17 I. H. Lin, C. C. Cheng, Y. C. Yen and F. C. Chang, *Macromolecules*, 2010, **43**, 1245.
18 N. E. Botterhuis, D. J. M. van Beek, G. M. L. van Gemert, A. W. Bosman and R. P. Sijbesma, *J. Polym. Sci., Part A: Polym. Chem.*, 2008, **46**, 3877.
19 C. C. Cheng, C. F. Huang, Y. C. Yen and F. C. Chang, *J. Polym. Sci., Part A: Polym. Chem.*, 2008, **46**, 6416.
20 S. H. M. Söntjens, R. A. E. Renken, G. M. L. van Gemert, T. A. P. Engels, A. W. Bosman, H. M. Janssen, L. E. Govaert and F. P. T. Baaijens, *Macromolecules*, 2008, **41**, 5703.
21 J. Wu, W. Pisula and K. Müllen, *Chem. Rev.*, 2007, **107**, 718.
22 G. ten Brinke, J. Ruokolainen and O. Ikkala, *Adv. Polym. Sci.*, 2007, **207**, 113.
23 B. Gong, W. Kim and C. Y. Ryu, *Angew. Chem., Int. Ed.*, 2004, **43**, 6471.
24 T. Park and S. C. Zimmerman, *J. Am. Chem. Soc.*, 2006, **128**, 13986.
25 H. Kautz, D. J. M. van Beek, R. P. Sijbesma and E. W. Meijer, *Macromolecules*, 2006, **39**, 4265.
26 P. Y. W. Dankers, Z. Zhang, E. Wisse, D. W. Grijpma, R. P. Sijbesma, J. Feijen and E. W. Meijer, *Macromolecules*, 2006, **39**, 8763.
27 A. Chen, D. Wu and C. S. Johnson Jr., *J. Am. Chem. Soc.*, 1995, **117**, 7965.
28 P. J. Flory, *J. Chem. Phys.*, 1949, **17**, 223.
29 F. S. Bates and G. H. Fredrickson, *Annu. Rev. Phys. Chem.*, 1990, **41**, 525.
30 R. P. Sijbesma, F. H. Beijer, L. Brunsveld, B. J. B. Folmer, J. H. K. Ky Hirschberg, R. F. M. Lange, J. K. L. Lowe and E. W. Meijer, *Science*, 1997, **278**, 1601.
31 V. G. H. Lafitte, A. E. Aliev, P. N. Horton, M. B. Hursthouse, K. Bala, P. Golding and H. C. Hailes, *J. Am. Chem. Soc.*, 2006, **128**, 6544.
32 E. Rabani, D. R. Reichman, P. L. Geissler and L. E. Brus, *Nature*, 2003, **426**, 271.
33 C. E. Atkinson, A. E. Aliev and W. B. Motherwell, *Chem.–Eur. J.*, 2003, **9**, 1714.
34 A. Jerschow and N. Müller, *J. Magn. Reson.*, 1997, **125**, 372.